

Treating the case of incurable hysteresis in VO₂

M. Gurvitch^{a,b}, S. Luryi^{a,c}, A. Polyakov^a, A. Shabalov^a

^a*NY State Center for Advanced Sensor Technology (Sensor CAT),* ^b*Dept. of Physics and Astronomy,*

^c*Dept. of Electrical and Computer Engineering SUNY at Stony Brook, Stony Brook, NY 11794, U.S.A.*

1. Introduction

Phase transitions present an opportunity for a useful application utilizing a natural proximity of two phases with different physical properties and an ability to trigger the transition by varying a transition-controlling parameter, such as temperature, or magnetic field, etc. There exist applications based on magnetic transitions, optical transitions, metal-insulator transitions, superconducting transitions. Some of these phase transitions, especially those classified as *first order* transitions (i.e. accompanied by the release or absorption of latent heat), are hysteretic in nature, so that the two phases transform into each other along different routes depending on the direction of change of a transition-controlling parameter. The hysteresis can be essential for an application. A well known example (in this case, of a hysteretic *second order* transition) is a ferromagnetic material which can be magnetized in an external magnetic field and, because of the hysteresis, will remain magnetized when the external field is reduced to zero. This is used for making permanent magnets and in magnetic storage of information. The stored, “memorized” magnetization can be erased, which requires specific steps to be taken, such as going around the magnetic hysteresis loop with diminishing external fields. In other cases, however, the utilization of a phase transition is hindered by its hysteresis. The “memory” of the previous history that is beneficial in magnetic materials may become detrimental in other applications, where the irreversible (or, more precisely, not easily reversible) change in a given material’s property, e.g. resistivity, may be undesirable.

In this paper we consider VO₂, a material undergoing first order phase transition, and refer to an application -- IR visualization utilizing resistive bolometers made of VO₂ -- in which hysteresis causes problems. We offer a way of operation which circumvents these problems. The applied aspects of IR visualization vis-à-vis our proposed approach are discussed in our recent publication^[1], and we will refer to it in a number of instances for further details and references. Here we want to explain the essence of the method and touch upon its physics fundamentals.

2. Hysteretic semiconductor-metal phase transition in VO₂; major and minor loops.

In VO₂ resistivity changes by 3-5 orders of magnitude in a spectacular semiconductor-to-metal phase transition around 68 C^[2]. In addition to resistivity,

other properties change in this 1-st order phase transition, including crystalline structure and optical constants. In single crystals the transition is very sharp, with hysteresis width of only 1-2 °C^[3]; however, in polycrystalline films it is broader, with hysteresis width (as measured in the middle of a transition) of 10-20 °C. The resistive transition measured in one of our VO₂ films can be seen in Figs. 1-4 (look at the outside *major* loop; ignore for now the inner or *minor* loops or their parts which are shown on these figures). The films used in these measurements were prepared on Si/SiO₂ substrates by Pulsed Laser Deposition; details of sample preparation and measurements can be found in Ref. 1. On the log(R) vs. T plot, starting from room temperature, with increasing T resistivity first follows the semiconducting S-phase slope, then falls sharply along the right (heating) branch of the transition reaching metallic M-phase; the decreasing temperature corresponds to values of R tracing the left (cooling) branch, eventually forming a closed loop between two transition-end points T_S and T_M. As can be seen in Figs. 1-4, resistivity below the transition, in the S-phase, is about 3 orders of magnitude higher than that above the transition, in M-phase. The hysteresis width in the middle of this log(R) vs. T plot is about 15 °C, while the total width of a hysteretic region is T_M – T_S ≈ 50 °C.

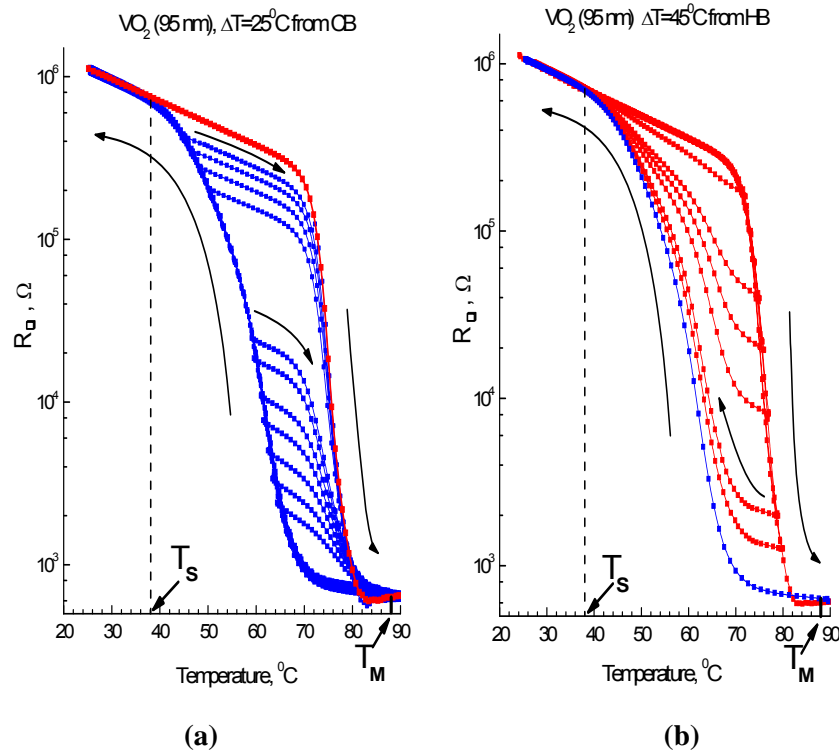


Figure 1. Major hysteresis loop of VO₂ film with a number of minor loops initiated from various temperatures T_0 on **(a)** the cooling branch, $T_0 \rightarrow T_0 + \Delta T \rightarrow T_0$, $\Delta T = 25$ °C, and **(b)** the heating branch, $T_0 \rightarrow T_0 - \Delta T \rightarrow T_0$, $\Delta T = 45$ °C.

For a variety of reasons, of the many proposals to use this transition in applications almost none materialized. One commercial and military application in which the use of VO_2 was initially envisioned is IR visualization (night vision) based on resistive microbolometers. However, technology eventually settled on a VO_2 -s poor cousin, a non-transitioning mixed oxide VO_x , mainly to avoid hysteresis, which greatly complicates bolometer operation, as was mentioned in the introduction and will be discussed in more detail below.

The major loop encompasses all the points on the (T, R) plane which can serve as starting points of minor hysteresis loops. In particular, minor loops can be initiated at any point along the outer lines of the major loop. In Fig. 1 we show several minor loops which were traced by reversing the temperature change at various points along the major loop: in Fig. 1a, minor loops are starting along the points of the cooling branch (CB); in Fig. 1b: along the points of the heating branch (HB). The loops shown in Fig. 1 cover wide temperature ranges of 25 °C in 1a and 45 °C in 1b. A number of minor loops traced over a more narrow temperature range of 10 °C are shown in Fig. 2.

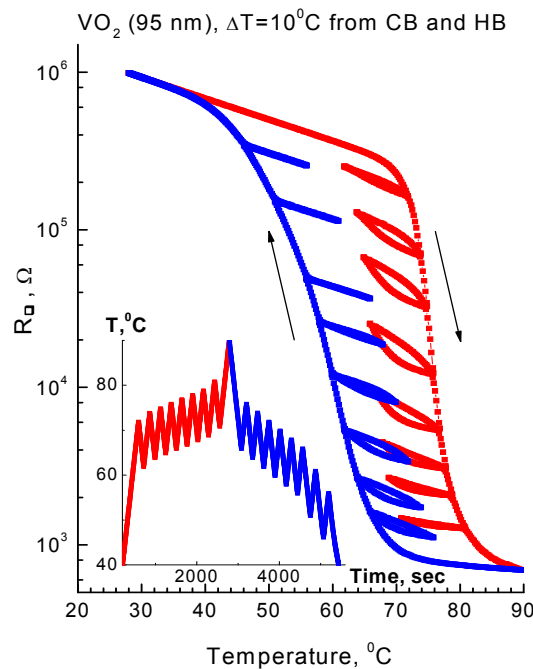


Figure 2. Minor loops with $\Delta T = 10^\circ\text{C}$; the inset shows the way in which temperature was changed in this measurement.

3. How hysteresis causes problems in bolometric readout; forward and backward excursions.

A bolometer reacts to a temperature change ΔT by changing its resistance by ΔR . The larger is ΔR for a given ΔT , the greater is the sensitivity. At the same time,

very large resistance R is detrimental because of bolometric sensor Joule heating during readout, difficulty of matching to the electronic readout circuit and higher noise, both Johnson and $1/f^{[1]}$. Thus a commonly-used measure of the bolometric material's sensitivity is the logarithmic derivative $(1/R) \Delta R/\Delta T$ called temperature coefficient of resistance, or TCR. In other words, it is not the high ΔR but high $\Delta R/R$ which is desired.

The steep semiconductor to metal transition seem to promise great sensitivity (high TCR), comparable to the sensitivity which can be achieved in a transition-edge superconducting sensor, which provided the original incentive to employ such a transition in VO_2 ^[4]. Why then was it not used? The main reason it was not used is because of hysteresis.

Let us look in more detail on how hysteresis causes problems. To be specific, let us consider a bolometer positioned at a working point (T_0, R_0) on a steep heating branch (HB) (it will require a temperature controller to keep it at T_0 above room temperature) and let it experience an influx of energy (this could be an IR signal) which momentarily heats it up, increasing its temperature by ΔT and decreasing its resistance by a large ΔR (Fig. 3).

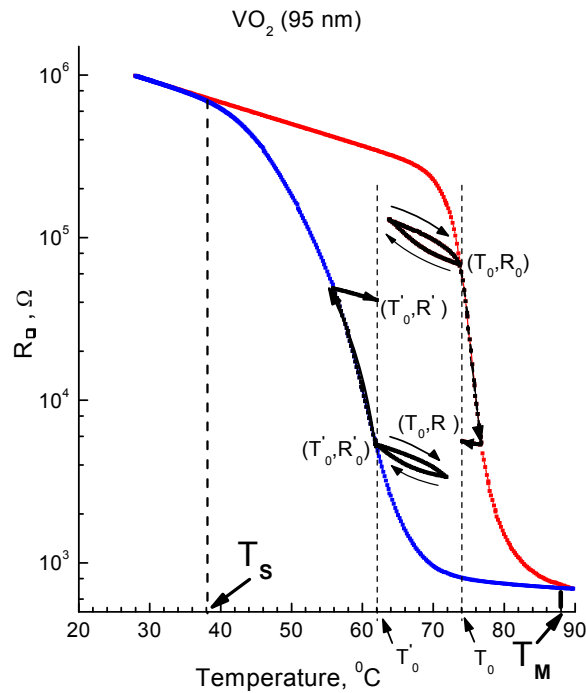


Figure 3. Forward excursions originating from point (T_0, R_0) on a HB and from point (T'_0, R'_0) on a CB, tracing open curves ending at (T_0, R) on a HB and at (T'_0, R') on a CB. The backward excursions from (T_0, R) and (T'_0, R') return to the points of their origin following closed minor loops. Note that this figure is not a schematic drawing; it shows measured loops and parts of loops.

Once the heat input has been removed (which happens in resistive bolometers used in IR visualization at least 30 times per second), the bolometer returns back to the temperature T_0 ; however, because of the hysteresis, the (T, R) path on the way back differs from the path in the forward direction: the resistance will not come back to R_0 , but instead will move along the part of the *minor* loop to a point (T_0, R) as indicated in Fig. 3. If a bolometer will now experience a subsequent, second heat pulse, the result will be very different. This can not be tolerated in a bolometric sensor subject to a train of pulses. In order to avoid this problem the bolometer should be reset after each pulse, which can only be done by going all the way out of the hysteresis loop, reaching temperatures either below T_S or above T_M , as can be seen in Fig. 1. While such resetting can be done, it requires large temperature *excursions* (we will call a round-trip temperature change $T_0 \rightarrow T_0 \pm \Delta T \rightarrow T_0$ an *excursion*) followed each time by temperature stabilization at the working point T_0 . With bolometers receiving signals with frequency of 30-60 Hz (video rates) this is not practical. The problem with the different return path we just outlined has been described in the literature^[5], and the readout problems caused by hysteresis were acknowledged^[6] as the major contributing factor in killing the original proposal^[4] of using high TCR found in a VO_2 transition.

A word about terminology: as was said, we call a round trip $T_0 \rightarrow T_0 \pm \Delta T \rightarrow T_0$ an *excursion*. We consider *excursion* length ΔT a positive quantity, and show the plus or minus sign in front of it explicitly. If temperature of the initial part of an excursion changes in the same direction as the major loop progression, we call it a *forward excursion*; if it starts in the opposite direction, it is a *backward excursion*. Thus in Fig. 3 on the HB the excursion from (T_0, R_0) to (T_0, R) is a forward one; the other one, forming a closed loop, is a backward one. We could discuss similar processes originating from a point (T'_0, R'_0) on a CB (they are also shown in Fig. 3), keeping in mind that on a CB decreasing temperature corresponds to the forward direction, and increasing temperature to the backward direction.

Because of the hysteresis, forward and backward excursions produce dramatically different results. While a forward excursion $T_0 \rightarrow T_0 + \Delta T \rightarrow T_0$ on a HB traces an open curve from (T_0, R_0) to (T_0, R) , a backward excursion $T_0 \rightarrow T_0 - \Delta T \rightarrow T_0$ produces a closed minor loop, which has a much smaller slope near (T_0, R_0) than the steep slope on the major loop, this slope increasing for larger ΔT , as can be seen in Fig. 3 and as can be inferred from Fig. 1. This will introduce signal non-linearity in $\log(R)$ vs. T , involving changing TCR which depends on the value of ΔT . Similar processes take place on a CB (Fig. 3).

To summarize, hysteresis causes the following two distinct types of problems:

- Forward excursions produce open (T,R) curves (“memory” effects), which are un-acceptable in a bolometer operating in a regime of repeating, multiple measurements.
- Backward excursions produce closed loops, so that bolometer re-setting is not required. However, the double-valued nature of such a minor loop makes readout ambiguous, and variable TCR found in minor loops is unacceptable, or at least detrimental, producing non-linearity in the

bolometric response, with small ΔT corresponding to smaller TCR, larger ΔT to larger TCR.

4. Non-hysteretic branches (NHB) in resistivity

Let us examine Fig.2 in more detail. We see that most of the minor loops in Fig. 2 are hysteretic, but we also notice that some of them are rather flat, single-valued, particularly those near the major loop ends T_S and T_M . In studying minor loops with progressively smaller excursions ΔT we discovered that for sufficiently small ΔT minor loops flattened out, degenerating into what we call *non-hysteretic branches* (NHB's). Although some minor loops become flat with $\Delta T = 10^\circ\text{C}$ (Fig. 2), all of them become flat at or below $\Delta T_{\text{NHB}} = 4^\circ\text{C} - 5^\circ\text{C}$, as can be seen in Fig.4:

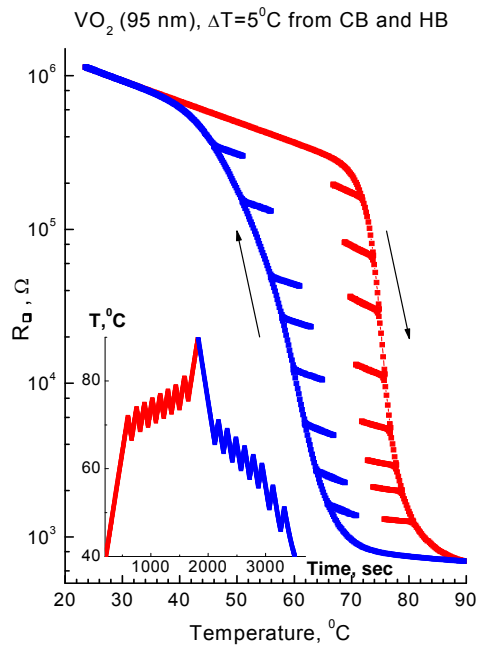


Figure 4. Minor loops with $\Delta T = 5^\circ\text{C}$; the inset shows the way in which temperature was changed in this measurement.

A NHB can be initiated from any point on the major loop, either on a HB or on a CB; NHB-s are linear in $\log(R)$ vs. T with negative slopes (semiconducting TCR-s). Two representative NHB-s measured in round-trip excursions are plotted on $\ln(R)$ vs. T scales in Fig. 5a, b.

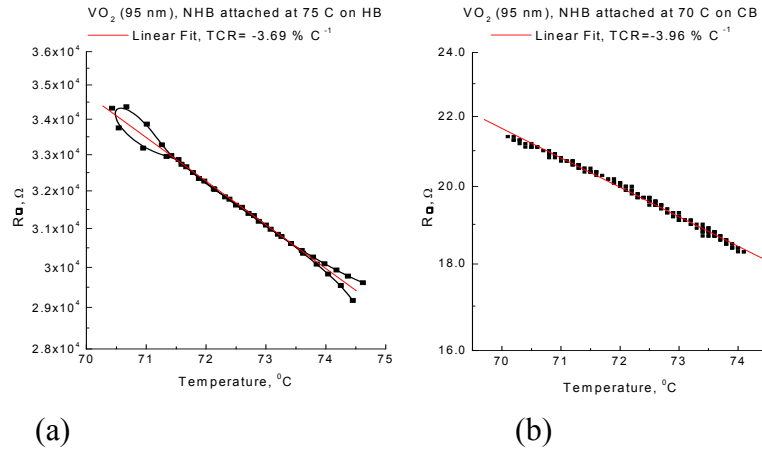


Figure 5. (a) NHB attached to the HB, with $R_{\square} \approx 31 \text{ k}\Omega$; $\text{TCR} = -3.69 \text{ \% } ^\circ\text{C}^{-1}$; **(b)** NHB attached to the CB, with $R_{\square} \approx 20 \text{ }\Omega$; despite this low resistance, $\text{TCR} = -3.96 \text{ \% } ^\circ\text{C}^{-1}$

NHB-s are single valued to the precision of our measurements, except for the temperature intervals near the attachment point T_0 and the turning point $T_0 \pm \Delta T$, where they sometimes appear double-valued, exhibiting a small loop and a fork, as seen in Fig. 5a. These features depend on the rate of temperature sweep; they are probably instrumental effects resulting from a lag between film surface and thermometer temperatures^[1].

TCR-s of various NHB-s from Fig. 4 are plotted vs. T_0 in Fig. 6 for both HB and CB.

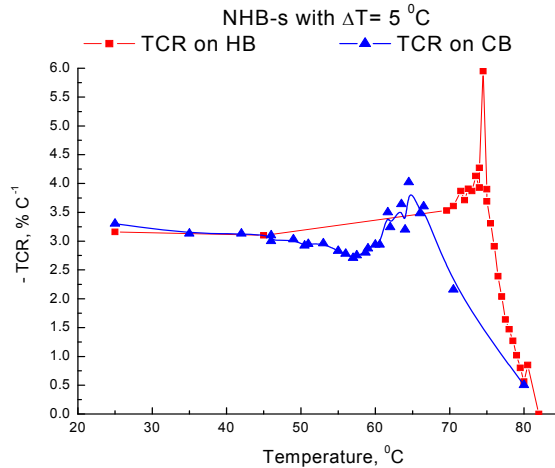


Figure 6. Absolute values of TCR plotted versus T_0 for various NHB-s around the major loop.

The S-phase $(\text{TCR})_S$ at 25 C is $3.3 \% \text{ } ^\circ\text{C}^{-1}$, which is considerably higher than a typical $\text{TCR} \approx 2 \% \text{ } ^\circ\text{C}^{-1}$ at 25 °C found in the literature on VO_x [1,6]. In an intrinsic semiconductor $E_g = 2(|\text{TCR}|)k_B T^2$ [1], and substituting $|\text{TCR}| = 0.033$ and $T = 25 + 273.1 = 298.1 \text{ K}$, we obtain $E_g = 0.51 \text{ eV}$, in fair agreement with the bandgap value in VO_2 single crystals [3].

As we see in Fig. 6, NHB-s logarithmic slopes are peaking at 65 °C on the CB and 75 °C on the HB, with maximum values of $4\% \text{ } ^\circ\text{C}^{-1}$ and $6\% \text{ } ^\circ\text{C}^{-1}$, decreasing sharply above the peaks. We note that the highest TCR-s on the sides of the major loop are found at the same temperatures.

5. Theoretical model

We will present a theoretical model which provides a qualitative explanation of the observed behavior and, moreover, has predictive power. Specific predictions made with our model will be put to a test by comparing them to experiment in the next section.

The hysteretic region in VO_2 is a mixed state consisting of both the S-phase and M-phase regions, or domains. Each such region located in a film around a point with spatial coordinates (x, y) transitions into the other phase at its own temperature $T_C(x, y)$, the variation in T_C arising from non-uniformities of composition, variations in the local strain, etc. Thus in a macroscopic sample $T_C(x, y)$ is quasi-continuously distributed. We assume that the local transition within a domain is sharp; further, we assume that a uniform isolated domain would transition without a hysteresis; in this we differ from much of the VO_2 hysteresis literature [7] in which it is usually assumed that each domain, in addition to T_C , has its own coercive temperature and a rectangular hysteresis loop. In contrast, we do not see a need for postulating such intrinsic hysteresis in isolated domains. We note that single crystals have very small hysteresis [3]; it seems natural to extrapolate this to the case of an ideally-uniform microscopic (or nanoscopic) region which would have zero hysteresis. In our picture hysteresis is the result of interaction between different phases in a multi-domain macroscopic sample, as will be detailed below.

At a given temperature T inside the major hysteretic loop, some parts of the film have $T_C(x, y) < T$ and some $T_C(x, y) > T$. In the first approximation, the boundary wall between the S and M phases is determined by the condition $T_C(x, y) = T$. In this approximation, the wall is highly irregular and its ruggedness corresponds to the scale at which one can define the local $T_C(x, y)$, i.e. to the characteristic length scale of the nanoscopic phase domains. On closer inspection, however, we need a refinement that takes into account the *boundary energy*, associated with the phase domain wall itself. The boundary energy is positive and to minimize its contribution to the free energy the domain walls are relatively smooth.

Let us examine the process of boundary motion. For concreteness, let us consider the heating branch. Below the percolation transition, M phase resembles lakes in

the S phase mainland. With raising temperature the area of the M phase increases, lakes grow in size. When a boundary of a given lake is far from the other lakes, infinitesimal $\pm dT$ changes boundary length by infinitesimal amount $\pm dL$, and the lake area by $\pm dA_M$. In other words, when the lakes are sufficiently separated, we envision a continuous, reversible, hysteresis-free process of $M \leftrightarrow S$ area redistribution, with neighboring configurations differing *microscopically*, what we call *area breathing*.

Let us now look at the formation of a link between two neighboring regions, which is the elementary step in the topological evolution of a global percolation picture. Let us focus on two metallic lakes that are about to merge. Since the boundary is smooth, at some temperature the distance between the lakes becomes smaller than the radius of curvature of either lake at the point they will eventually touch. Therefore, at some $T = T_{cr}$ the following two configurations will have equal energies: one comprising two disconnected M phase lakes that are near touching, but not quite, and the other with a finite link formed, Figs. 7a and 7b respectively.

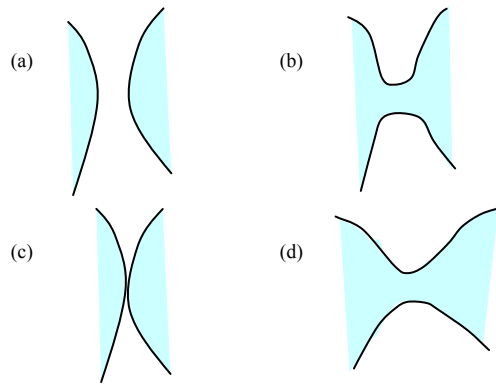


Figure 7. Semiconductor-metal boundary; metallic phase is shown shaded. Top row (a), (b) corresponds to temperature T_1 and the bottom row (c), (d) to temperature $T_2 > T_1$.

Both configurations are characterized by equal boundary lengths and therefore have equal free energy. In the thermodynamic sense one could call the T_{cr} the critical temperature for the link formation, if we could wait long enough. The actual transition forming a local link, however, does not occur at that temperature because of an immense *kinetic* barrier between these two *macroscopically* different configurations. The transition occurs at a higher $T_0 = T + \Delta T^*$ when it is actually forced, i.e. when the two phases touch at a point. Here ΔT^* is the *coercive* temperature. As can be seen, in our picture coercive temperature arises as a result of having a boundary between different phases; it does not pre-exist intrinsically within each domain. We associate the steep slopes of the major loop with the quasi-continuous formation of such links, i.e. with local topological changes, specifically with the merger of metallic lakes on the HB and semiconductor lakes

on the CB. Near T_S and T_M the global map consists of widely-separated M and S lakes, respectively. In these regions we expect to see non-hysteretic behavior; indeed, looking at Fig. 3 we see that $\Delta T = 10^\circ\text{C}$ NHB-s are largely non-hysteretic within $\approx 20^\circ\text{C}$ from T_S and $\approx 15^\circ\text{C}$ from T_M .

Consider now a small excursion backwards from T_0 on the HB. As the temperature decreases, some of the M-phase recedes and the S-phase grows, changing the geometry of the global two-phase map. However, topologically, the last formed M-link does not disappear immediately for the same kinetic reason. One has two S regions that need to touch in order to wipe out the M-link. It takes a backward excursion of amplitude ΔT^* to establish an S-link and thus disconnect the last M-link. So long as we are within ΔT^* , i.e. stay on the same NHB, the area of S and M domains changes continuously, but the topology is stable and no new links are formed. Within the range of that stable or *frozen topology*, $\Delta T^* = \Delta T_{\text{NHB}}$, the resistivity of NHB will be single-valued and its T-dependence will be controlled by the percolating semiconductor phase. This explains why NHB-s have semiconducting slopes.

We introduced here a notion of *frozen topology*, which describes a global two-phase map with stable connecting links between regions of the same phase, while geometrical shape of the two phases is allowed to change, or *breathe*. One can also envision NHB-s in which *breathing* stops altogether, no switching between phases taking place, keeping the geometrical outlines fixed, this being the case of *frozen geometry*. Clearly *frozen geometry* implies *frozen topology*, but not the other way around. We will see below that both conditions actually exist and can be observed in a transitioning VO_2 .

We can further address the observed phenomenon of TCR enhancement in some of the NHB-s, where TCR-s exceed the S-phase value (Fig.6). We note that for all NHB-s, on both branches of the major loop, higher T implies increased fraction of M-phase, even if no new links are formed. This smooth change in geometry will produce additional T-dependence adding to the semiconductor slope within a NHB, i.e. higher TCR. This effect will be stronger in the temperature intervals where this smooth change in geometry is more active, and it will cease to exist in the regions of *frozen geometry*, where NHB slope will be determined only by the percolating S-phase. We will refer to this effect vis-à-vis optical data below.

Theoretical models which explain the data are good, but those which correctly predict new behavior are better. What can we predict based on our model?

We recall that hysteresis takes place in all physical properties which change in the phase transition. In addition to resistivity, optical constants, such as refractive index n , change in the VO_2 transition. In a small uniform domain n changes abruptly at T_C , from n_S to n_M ; in a macroscopic film there is a distribution of $T_C(x,y)$ and therefore, in a temperature range of co-existing S and M phases, $T_S < T < T_M$, there will be some S domains with n_S and some M domains with n_M . As phases transform with changing T, there will be a temperature dependent hysteretic $n(T)$ in a macroscopic film, much like previously discussed $R(T)$. Indeed, optical

properties exhibit hysteretic transition as a function of temperature. Among them, optical reflectivity is probably the easiest optical quantity to measure; the details of how optical reflectivity behaves in a phase transition in a film with thickness comparable with the wavelength of light have to do not only with $n(T)$ but also with thin-film interference; this was discussed in Ref. 8 (and in references therein), and we will not repeat the explanation here. The result is that, when T increases from 25 C to 100 C and decreases back to 25 C, optical reflectivity $R_\lambda(T)$ at a fixed wavelength λ traces a hysteresis loop between certain values $R_{\lambda S}$ and $R_{\lambda M}$, these values being determined by a number of factors, including the choice of λ , film thickness, n_S and n_M . We can further expect that backward excursions from the points on the major optical loop will produce optical NHB-s, for the same reason they exist in $R(T)$, and indeed we observed them, as will be seen below.

Based on our theoretical model, what specific behavior can we predict in optical reflectivity vs. T ? Reflectivity is measured at wavelengths exceeding the nano-domain scale. It is largely determined by thin-film interference, with two-phase material between the film surfaces (in the Fabry-Perot resonator) having the average value of n , the latter depending on the volume fraction of S and M phases (volume fraction of n_S and n_M), which in a thin film becomes the area fraction of the two phases. In contrast, resistivity depends on the connectivity (links) of the percolating phase. Let A_S and A_M be the areas of S-phase and M-phase in a two-dimensional sample (thin film), so that the total sample area is $A = A_S + A_M$. Clearly, as A does not depend on T , $dA_M/dT = -dA_S/dT$, i.e. the area of one phase grows at the expense of the other. The optical slope dR_λ/dT observed in optical NHB must be proportional to this area re-distribution slope, with the maximum in dR_λ/dT reflecting the maximum in dA_M/dT . According to our explanation of TCR enhancement over the S-phase value, the highest TCR should be found at the point which has the highest rate of area re-distribution $dA_M/dT = -dA_S/dT$, and, therefore, at the point which corresponds to the maximum optical NHB slope dR_λ/dT . Likewise, zero rates of area re-distribution (*frozen geometry*) corresponding to $dR_\lambda/dT = 0$, should correspond to un-enhanced S-phase TCR. In the next section we will have a chance to verify these specific predictions.

The percolation picture also helps to understand why dR_λ/dT will exhibit such a maximum in the first place. With changing temperature, the boundary moves, each section of the boundary line advancing in the direction normal to this line at any given temperature. It is clear that the highest rate of change of the area of each phase will therefore occur when the boundary is the longest, i.e. at the percolation transition. If our picture is correct, then the observed peak in TCR vs. T_0 in Fig. 6 occurs right at the percolation transition, allowing its detection. Finally, we see in Fig.6 that above the peak, i.e. above the percolation transition, TCR-s are quickly decreasing. Indeed, if the M-phase percolates, it is shorting out the S-phase, and such decrease is to be expected.

6. NHB-s in optical reflectivity: testing the theoretical model

In order to test some of the predictions of our model, simultaneously with the resistive measurements presented above in Figs. 2 and 4, we measured reflectivity at a fixed wavelength λ , $R_\lambda(T)$. Optical signal was taken from the space between the voltage probes used in 4-probe resistivity measurement. In Fig. 8 we show major loop and minor hysteresis loops with $\Delta T = 10^\circ\text{C}$ in optical reflectivity $R_\lambda(T)$ (i.e. this is an optical analog of Fig. 2).

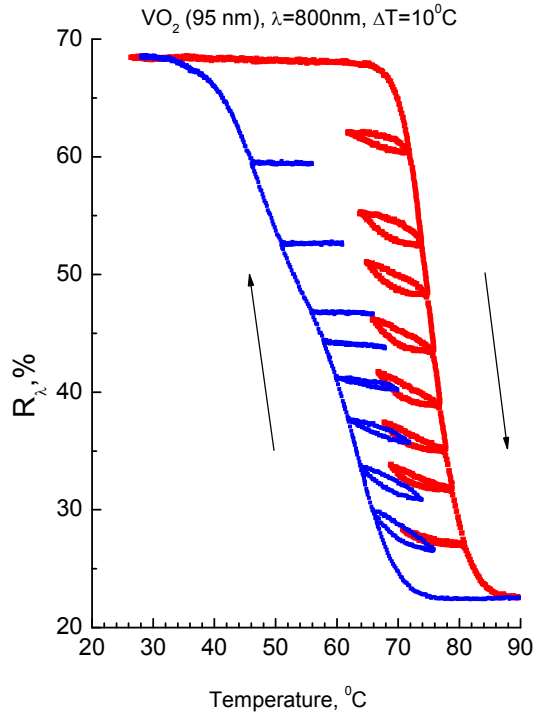


Figure 8. Major hysteresis loops in optical reflectivity with minor loops, excursion length $\Delta T = 10^\circ\text{C}$, measured at $\lambda = 800\text{ nm}$.

In Fig. 8 we see minor loops, some of them degenerating into optical NHBs, just like in resistivity in Fig. 2. Additionally we see that some minor loops are T-dependent, while others are not, and that T-dependent ones tend to be double-valued loops, while T-independent ones are degenerating into NHB-s. In Fig. 9 we plot data for the same sample with short 5°C excursions (i.e. this figure is an optical analog of Fig. 4).

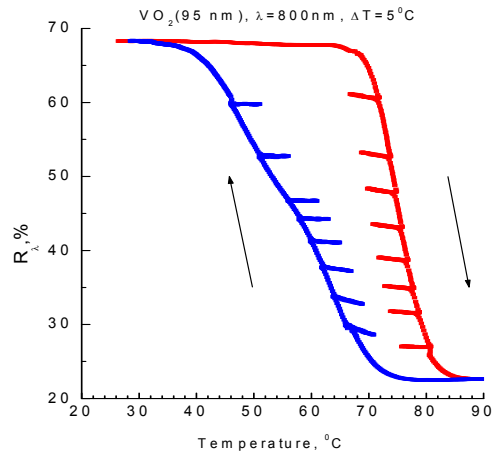


Figure 9. Data as in Fig. 8, but with $\Delta T = 5^\circ\text{C}$.

We see that all minor loops degenerated into NHB-s, in complete analogy to Fig. 4, and according to our expectation expressed in sec. 5. Some of these NHB-s, those closer to the center of the major loop, are T-dependent, the others, those closer to the loop limits, are not. The T-dependent ones correspond to hysteretic minor loops in Fig. 8, while T-independent NHB-s correlate with non-hysteretic behavior in Fig. 8.

Optical slopes dR_λ/dT of NHB-s from Fig.9 are plotted alongside TCR-s from Fig.4 in the combined Fig.10, for both HB and CB.

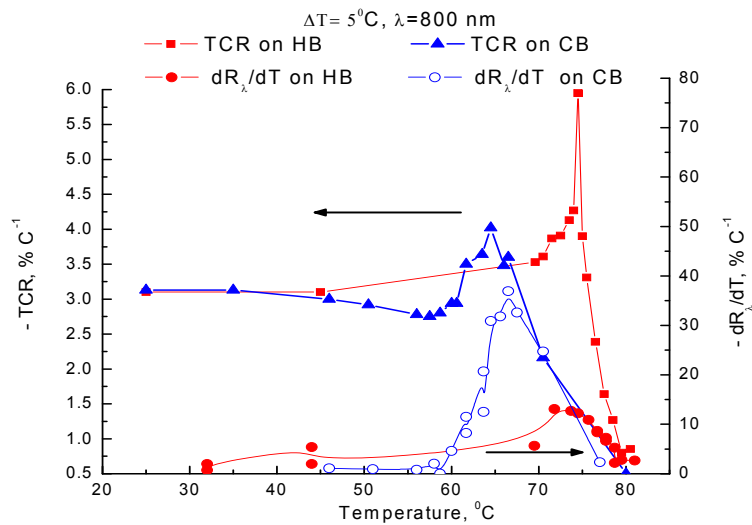


Figure 10. TCR-s and dR_λ/dT -s from various NHB-s around the major loop plotted on one graph, exhibiting expected correlations.

As can be seen, the specific predictions of our model are indeed proven true: the peaks in dR_λ/dT on both branches almost precisely coincide with the peaks in TCR, and the region in which $dR_\lambda/dT \approx 0$ corresponds to $TCR \approx (TCR)_S$. Further, if $dR_\lambda/dT \approx 0$ signifies *frozen geometry*, it is natural that in the absence of $S \leftrightarrow M$ transitions minor loops degenerate into NHB-s more readily, as is observed when we examine and compare Figs. 8 and 9. The small (≈ 2 degrees) misalignment of dR_λ/dT and TCR peaks which can be seen in Fig. 10 can be ascribed to the fact that the factors affecting the overall shape of the major optical loop, such as interference effects^[8], affect, at least to a degree, NHB slopes as well. Likewise, a relatively small deviation of TCR-s in the $dR_\lambda/dT \approx 0$ region from the S-phase value – the observed shallow TCR minimum on the CB – can be ascribed to secondary causes. We do not think that these details disprove or diminish the impressive overall agreement of the main features predicted by our model.

As was said above, the overall shape of the optical hysteresis and the range between pure-phase reflectivity values of $R_{\lambda S}$ and $R_{\lambda M}$ can be changed by making measurements at different wavelengths λ . We measured $R_\lambda(T)$ at two different λ ; the measurement at $\lambda = 800$ nm is shown in Figs. 8 and 9, and we also measured it at $\lambda = 503$ nm. The measurement at 503 nm produces an optical loop which looks entirely different than the one shown in Figs. 8 and 9. Yet we observed dR_λ/dT having the same peaks as seen in Fig. 10, these peaks correlating with TCR peaks, which strongly confirm that we are indeed observing intrinsic $S \leftrightarrow M$ area redistribution and not the effects of interference, etc.

Summing up, we proposed a theoretical picture, expressed in sec. 5 in qualitative terms, without detailed mathematical modeling, which would be rather involved (perhaps a task for the future). We describe hysteresis in the framework of a percolation transition, as arising from interaction of S and M phases, specifically ascribing strong hysteretic effects to link formation between the two phases. This model corresponds to a number of observed features in both resistive and optical data. The most impressive agreement is achieved in the explanation of a subtle effect of TCR enhancement over the S-phase value in a range of NHB-s where optical slopes correlate with TCR-s, leaving no doubt that we understand the reason for TCR enhancement correctly.

8. Resistive microbolometers in NHB regime

A detailed discussion of the NHB method in the context of IR visualization with resistive microbolometers (the Uncooled Focal Plane Array or UFPA technology) is given in Ref. 1. Here we only give a brief summary. Good quality, single phase VO_2 films will replace mixed oxide VO_x as sensor material in pixilated bolometric array. Despite using VO_2 , hysteresis is eliminated when a sensor array operates within a NHB. The NHB will be chosen on the basis of its desired resistance, which can be adjusted in a wide range in order to be matched to the readout circuit amplifier, and to be low enough to minimize noise and Joule heating. The resistance will be 2-3 orders of magnitude smaller than the unacceptably-high VO_2

resistance at 25 °C, while maintaining semiconducting TCR. We have seen NHB-s with resistance as low as 20 Ω having $\text{TCR} \approx -4\% \text{ } ^\circ\text{C}^{-1}$. NHB will be also chosen to maximize TCR, which, as we have seen, varies between different NHB-s around the major loop, peaking at the percolation transition, with values as high as $6\% \text{ } ^\circ\text{C}^{-1}$. The operating temperature T_{OP} (i.e. the temperature at which the sensor array is stabilized awaiting the projected IR signal) will be chosen within a NHB, either near one of the ends or in the middle of the available range (total NHB width) $\Delta T_{\text{NHB}} = 4\text{--}5 \text{ } ^\circ\text{C}$. Because of the hysteresis, the process of reaching T_{OP} starting from room temperature requires performing specific heating and cooling steps. Specifically, positioning an array at T_{OP} will require: on a HB, warming up to T_0 and cooling down to T_{OP} ; on a CB, warming up to above T_{M} , cooling down to T_0 , and again warming up to T_{OP} . If T_{OP} is chosen in the middle of a NHB, the last step requires cooling down from T_0 to $T_0 - \Delta T_{\text{NHB}}/2$ on a HB, and warming up from T_0 to $T_0 + \Delta T_{\text{NHB}}/2$ on a CB.

9. Summary

We found a regime of operation within a hysteretic phase transition which, within a limited range of a transition-controlling parameter, avoids hysteresis. This may benefit applications utilizing a phase transition but suffering from complications introduced by hysteresis. One such application is IR visualization with resistive microbolometers. We propose to use VO_2 as a sensor material, operating it in the non-hysteretic branch (NHB) regime. Partial shorting out of the S-phase by the M-phase lowers sensor resistance; the degree of admixture of M-phase determines the value of this resistance, making it adjustable. At the same time, because of the S-phase percolation, NHB has semiconducting $R(T)$. The TCR in this case can be considerably higher than in the pure S-phase due to a smooth change of geometry (but not the topology) of S-M areas within an NHB. A similar NHB regime exists in optical reflectivity. Optical reflectivity slopes correlate with TCR-s, revealing the reason for TCR enhancement in some of the NHB-s over the S-phase value. We believe that NHB regime may be implemented in any hysteretic phase transition, removing problems associated with hysteresis and potentially benefiting electronic applications.

Acknowledgements

We thank Dr. David Westerfeld for developing Lab View-based automated resistivity measurement system and Dr. Arsen Subashiev for useful theoretical discussions. This work was supported by the New York State Foundation for Science, Technology and Innovation (NYSTAR) through the facilities of the Center for Advanced Sensor Technology at Stony Brook.

References

1. M. Gurvitch, S. Luryi, A. Polyakov, A. Shabalov, “Non-hysteretic behavior inside the hysteresis loop of VO₂ and its possible application in infrared imaging”, *J. of Appl. Phys.* **106**(8), (2009).
2. F. J. Morin, *Phys. Rev. Letters* **3**, 34 (1959); N. Mott, “Metal-Insulator Transitions”, Taylor & Francis, London (1997).
3. C. N. Bergland and H. J. Guggenheim, *Phys. Rev.* **185** (3), pp. 1022-1033 (1969).
4. R. S. Scott and G. E. Frederics, “Model for Infrared Detection by a Metal-Semiconductor Phase Transition”, *Infrared Physics* **16**, pp. 619-626 (1976).
5. V. Yu. Zerov, Yu. V. Kulikov, V. N. Leonov, V. G. Malyarov, I. A. Khrebtov, and I. I. Shaganov, *J. Opt. Technol.* **66**(5), pp. 387-390 (1999).
6. B. E. Cole, R. E. Higashi, and R. A. Wood, *Proc. of the IEEE* **86**(8), p.1679, (1998).
7. T. G. Lanskaya, I. A. Merkulov, and F. A. Chudnovskii, *Sov. Phys. Solid State* **20**(2), 193 (1978) and a number of subsequent references treating hysteresis in VO₂.
8. M. Gurvitch, S. Luryi, A. Polyakov, A. Shabalov, M. Dudley, G. Wang, S. Ge, V. Yakovlev, *J. Appl. Phys.* **102**, 033504 (2007).